

MODELING A MICROWAVE CATHETER ANTENNA FOR CARDIAC ABLATION

Ahmed Khebir, Zouheir Kaouk, and Pierre Savard

Institute of Biomedical Engineering Ecole Polytechnique and Université de Montréal
C. P. 6128, Succ. Centre-ville, Montreal, Quebec, Canada H3C 3J7**Abstract**

This article studies the possibility of using microwave energy for cardiac ablation as an alternative to RF energy since the latter has several clinical limitations. For this endeavor, a computer code, based on the powerful finite element method, was developed and used to design a prototype circular microwave catheter antenna; its volume heating was studied and compared to that of an RF electrode of similar dimensions and found that the former yields a lesion size as twice as large as the latter while respecting most of the clinical considerations.

Introduction

Recently, RF catheter ablation has become a widespread technique to treat tachycardia which is basically an abnormal increase in the heart rate[1]. The success rate of this procedure is as high as 95% for certain types of arrhythmias such as the Wolff-Parkinson-White (WPW) syndrome; however, it is much lower (10-50%) for some other types such as ventricular tachycardia occurring after myocardial infarction. This low success rate can be partly attributed to the size of RF lesion which is limited by the peak tissue temperature. It was found [2] that when tissue temperature exceeds 100 °C, boiling occurs and a thrombus is formed around the electrode which increases the impedance of the electrode/tissue interfaces, resulting in a decreased RF current flow. In addition, RF current lines are concentrated at the tip, and not along the length of the electrode. Finally, the arrhythmogenic substrate may be located near scar tissue in patients with old myocardial infarction and the altered electrical conductivity of the scar may divert the RF currents.

In contrast to heating with RF conduction currents, heating with microwaves is due to the propagation of electromagnetic waves that raise the energy of the molecules through which the wave passes by both conduction and displacement currents [3]-[4]. Consequently, a microwave antenna could, in principal,

deposit energy directly in tissue at a distance without being overtly affected by the intervening medium such as blood coagulum. Therefore, microwave antenna could potentially be designed to produce longer lesions that could more efficiently interrupt a reentry circuit in patients with ventricular tachycardia.

The purpose of this effort is to develop a computer code to be used for designing prototypes of microwave antennas and studying their volume heating for cardiac ablation applications. This necessitates a vector full wave electromagnetic analysis since the quasistatic approximation used for radio frequencies no longer holds for microwave frequencies. We carried out this task by using the finite element method (FEM) because it is well-suited for solving microwave problems for objects with complex structures and various material properties since it uses fully unstructured mesh.

THE NUMERICAL PROCEDURE

The shape of the heart is nearly axisymmetric. Therefore, we started our study by considering axisymmetric antennas since they are simpler to analyze as it is sufficient to perform a quasi-two-dimensional analysis on any arbitrary ϕ -plane. A general axisymmetric configuration of a microwave catheter embedded in a heart chamber is shown in Figure 1. The microwave energy is fed through the feedline into the antenna which, in turn, radiates it to the myocardium. The feedline extends from the microwave generator to the heart via an artery or a vein; obviously, it needs to be truncated at a close distance from the antenna to limit the size of the problem. An absorbing boundary condition is thus applied at that location -the input port- to account for the region which is not included in the finite element mesh.

The variational equation discretized by the finite element method is obtainable from the vector Helmholtz equation, along with the Galerkin's method:

TU
4E

$$F(\vec{W}, \vec{E}) = \int_V \left[\frac{1}{\mu_r} (\vec{\nabla} \times \vec{W}) \cdot (\vec{\nabla} \times \vec{E}) - k_o^2 \epsilon_r \vec{W} \cdot \vec{E} \right] dV - \int_{\Gamma} \left[\frac{1}{\mu_r} \vec{W} \times \vec{\nabla} \times \vec{E} \right] \cdot d\vec{S} \quad (1)$$

where V is the domain of computation, Γ is the boundary of the input port, \vec{E} is the electric field, and \vec{W} is the weighting function.

Since a purely nodal approach is known to poorly treat the spurious or the nonphysical modes, a hybrid node/edge approach is used instead. That is, a nodal representation for the azimuthal component and an edge element representation for the transverse component are used.

Taking advantage of the axisymmetry of the problem, the electric field can be assumed to have the following ϕ -dependence:

$$\vec{E}(\rho, \phi, z) = \vec{E}(\rho, z) e^{j\phi} \quad (2)$$

For any two-dimensional cut at a constant ϕ -plane, the electric field is decomposed into transverse and normal components to that plane as

$$\vec{E}(\rho, z) = \vec{e}_r(\rho, z) + \frac{e_r(\rho, z)}{\rho} \hat{\phi} \quad (3)$$

and the curl operator as

$$\vec{\nabla} = \nabla_r - \frac{j\omega}{\rho} \hat{\phi} \quad (4)$$

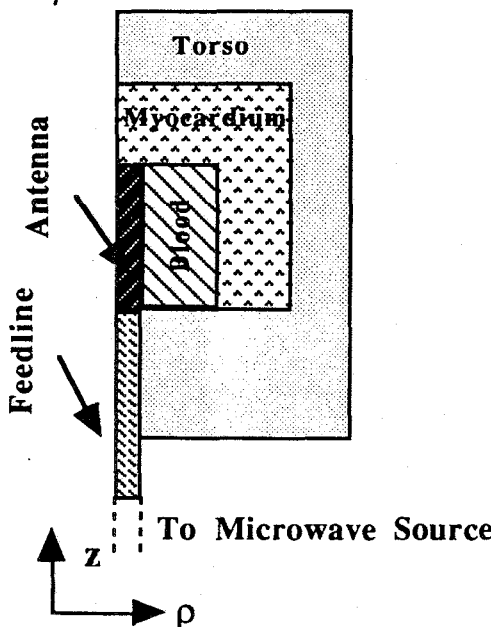


Figure 1: A Schematic representation of the model.

The surface integral term of equation (1) requires a special treatment because it involves a three-dimensional quantity to be represented on a two-dimensional cross section. In addition, the input port is the junction between the antenna and the feedline which is uniform and has a wave propagating along it. For a direction of propagation along z , the transverse component is in the x - y plane and the longitudinal component of the field is along z . As a result, the field and the curl decompositions in (3) and (4) are no longer valid to discretize the surface integral term. The following decompositions are, instead, used:

$$\vec{E} = (\vec{E}_{zr}(x, y) + \hat{z}E_r(x, y))e^{j\phi} \quad (5)$$

$$\vec{\nabla} = \vec{\nabla}_{zr} - \hat{z}j\beta \quad (6)$$

where β is the constant of propagation. Furthermore, the following absorbing boundary condition at the input port can be obtained [4]

$$\frac{\partial \vec{E}_{zr}}{\partial z} \Big|_{\text{input port}} = j\beta(\vec{E}_{zr} - 2\vec{E}_{zr}^{\text{inc}}) \Big|_{\text{input port}} \quad (7)$$

where $\vec{E}_{zr}^{\text{inc}}$ denotes the incident field.

Using the above equations, the following linear system of equations is obtained which can be solved for the electric field \vec{E} in the antenna, the myocardium, the blood, and the torso:

$$\begin{aligned} & \iint_s \frac{1}{\mu_r} \left\{ \left[\rho(\vec{\nabla}_r \times \vec{w}_r) \cdot (\vec{\nabla}_r \times \vec{e}_r) + \frac{m^2}{\rho} (\vec{w}_r \cdot \vec{e}_r) \right] \right. \\ & \left. - \frac{m}{\rho} [(\vec{w}_r \cdot \vec{\nabla}_r \vec{e}_r) + (\vec{\nabla}_r \vec{w}_r \cdot \vec{e}_r)] + \frac{1}{\rho} (\vec{\nabla}_r \vec{w}_r \cdot \vec{\nabla}_r \vec{e}_r) \right. \\ & \left. - \vec{\nabla}_r \cdot (\vec{w}_r \cdot \vec{e}_r) - k_o^2 \epsilon_r \mu_r \left[\rho(\vec{w}_r \cdot \vec{e}_r) + \frac{\vec{w}_r \cdot \vec{e}_r}{\rho} \right] \right\} d\rho dz \\ & + j\beta \int_r \frac{1}{\mu_r} [\vec{w}_r \cdot (\vec{E}_{zr} - 2\vec{E}_{zr}^{\text{inc}})] d\rho = 0 \end{aligned} \quad (8)$$

Note that at microwave frequencies, the conductivity and the permittivity of the myocardium and the blood strongly depend on the frequency. The empirical formulas given in [5] were used to include such dependence.

Equation (8) is solved for the electric field in the antenna, the myocardium, the blood, and the torso. The solution is fed to the steady-state heat conduction equation:

$$\begin{aligned} & \int_s \left\{ \frac{\partial N}{\partial \rho} k \frac{\partial T}{\partial \rho} + \frac{\partial N}{\partial z} k \frac{\partial T}{\partial z} - \frac{1}{2} N \sigma |\vec{E}|^2 \right\} d\rho dz \\ & + \int_{ce} \{1000 N(T - 37)\} \rho dl = 0 \end{aligned} \quad (9)$$

to obtain the temperature distribution in the domain of computation.

where N is nodal weighting function, T is the temperature distribution, and k is the thermal conductivity coefficient.

RESULTS AND DISCUSSION

The microwave catheter antenna should be designed so that it delivers sufficient microwave energy to produce irreversible tissue damage (i. e. a temperature higher than 48 °C) to a significant volume of the myocardium and, hence, to interrupt the path of the reentry circuit, but the power dissipated in the blood and the myocardium should remain below 40 Watts to avoid the possibility of damaging blood cells. The catheter should have a diameter of less than 3 mm since it is inserted into the heart via an artery or vein; its tip should be rounded to avoid injuring the vessel and the tissue; its dielectric filling ought to have a relatively high breakdown so as not to constrain the maximum electric field.

Figure 2 shows a detailed drawing of the catheter where the feedline is a homogeneously filled coaxial waveguide ($\epsilon_f = 2.1$) and the radius of its inner and outer conductors are 0.418mm and 1.4mm, respectively; thus, the characteristic impedance of the feedline is equal to 50 ohms which is the most commonly used commercial coaxial line. At the end of the coaxial feedline, there is a coaxial-monopole antenna where the distance $D_e = 3.0$ mm and its dielectric filling has relative permittivity $\epsilon_a = 20$; the whole catheter is covered with a dielectric sheath ($\epsilon_s = 12$). As mentioned earlier, our program calculates the conductivity and the permittivity of the myocardium and the blood from the empirical formulas given in [5] which suggest that the higher the frequency, the higher is loss and the sharper is the decay of the electromagnetic wave. Three different values of frequency were investigated, that is $f = 2, 4$, and 6 GHz. Table 1 shows the parameters associated with each frequency. Figure 4 shows the contour plot of the myocardial temperature distribution for a frequency of 4 GHz. A heating depth of 22.2mm is observed for this particular frequency.

Table 1

Simulation parameters for the cylindrical monopole antenna.

Freq. (GHz)	Lesion depth (mm)	R	P _i (W)	P _{db} (W)	P _{dm} (W)	ϵ_b	σ_b S/m	ϵ_m	σ_m S/m
2	15	0.41	24	12.6	4.9	55.4	1.4	47.5	1.41
4	22.2	0.11	34	27.0	5.19	54.0	2.8	46.2	2.62
6	16.5	0.35	87	66.5	4.2	52.4	5.0	44.8	4.44

|R|: reflection coefficient; P_i : incident power; P_{db} : power dissipated in the blood; P_{dm} : power dissipated in the myocardium; ϵ_b : blood permittivity; σ_b : blood conductivity; ϵ_m : myocardial permittivity; σ_m : myocardial conductivity.

To investigate the possible advantages of microwave energy with respect to RF energy, a simulation was performed using the RF model described in [1]. Figure 3 shows an RF electrode where its general shape and the dimensions (radius = 1.5 and distance $D_e = 3.0$ mm) are comparable to the microwave antenna shown in Figure 2. The conductivity of the blood, and the myocardium are equal to 0.67 and 0.5S/m, respectively. The power dissipated in the blood and the myocardium are equal to 3.23W and 1.98W, respectively. The temperature distribution is shown in Figure 5 where a heating depth of 10mm is obtained which is about half of the one obtained by the microwave antenna while the maximum tissue temperature remains at 100 °C. The greater heating depth predicted by our model for microwave energy is confirmed by experimental results obtained by Wonnell et al. using a myocardium-equivalent phantom model [3]. These theoretical and experimental results justify further studies on microwave catheter ablation.

CONCLUSIONS

We have presented a rigorous finite element approach to find the temperature distribution inside the heart chamber generated by a microwave catheter antenna for axisymmetric geometries. It was found that the microwave catheter antenna yields a sizable lesion that potentially would treat most types of arrhythmias while respecting most of the clinical considerations. In addition, such microwave antenna was proven to be superior to RF electrodes since the former yields a lesion roughly twice as large as the latter under similar operational conditions.

We are in the process of constructing this particular antenna so as to create *in vitro* lesions in canine models.

References

- [1] Z. Kaouk, A. V. Shahidi, P. Savard, and F. Molin, "Modeling of Myocardium Temperature during radiofrequency ablation," Submitted to Med. & Biol. Eng. & Computing.
- [2] D. E. Haines and D. D. Watson, "Tissue heating during RF catheter ablation: a thermodynamic model and observations in isolated perfused and superfused canine right ventricular free wall," PACE vol. 12, pp 962-, 1989.
- [3] T. L. Wonnell, P. R. Stauffer, and J. J. Langberg, "Evaluation of microwave and radio frequency catheter ablation in a myocardium-equivalent phantom model," IEEE Trans. Biomed. Eng., vol. 39, pp. 1086-1095, 1992.
- [4] R. M. Rosenbaum, et al., "RF and microwave ablation for the treatment of ventricular tachycardia" 1993

IEEE MTT-S International Microwave Symposium Digest, pp. 1155-1158, June 1993.

[5] K. R. Foster and J. L. Schepps, "Dielectric properties of tumor and normal tissues at radio through microwave frequencies," *J. Microwave Power*, vol. 16, pp.107-119, 10981.

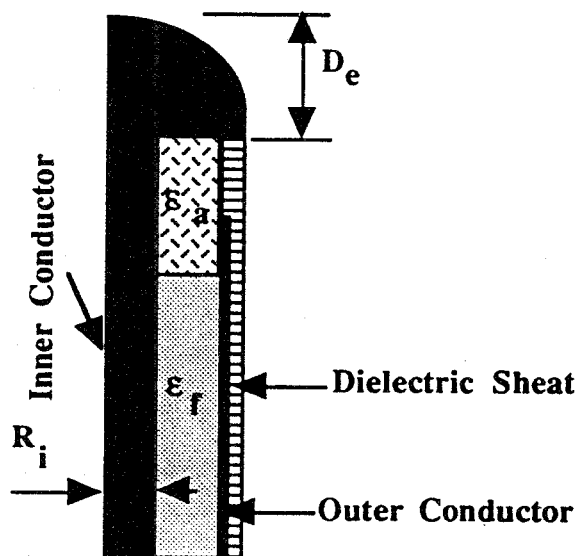


Figure 2: A Schematic representation of the microwave catheter antenna.

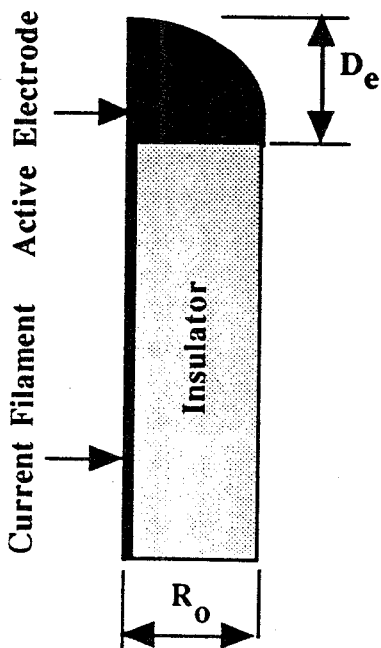


Figure 3: A Schematic representation of the RF electrode.

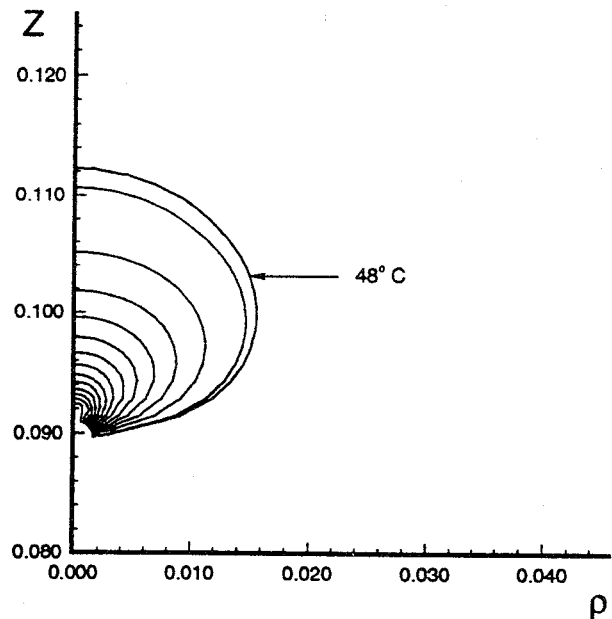


Figure 4: The temperature distribution in the myocardium produced by the microwave antenna configuration shown in Figure 2.

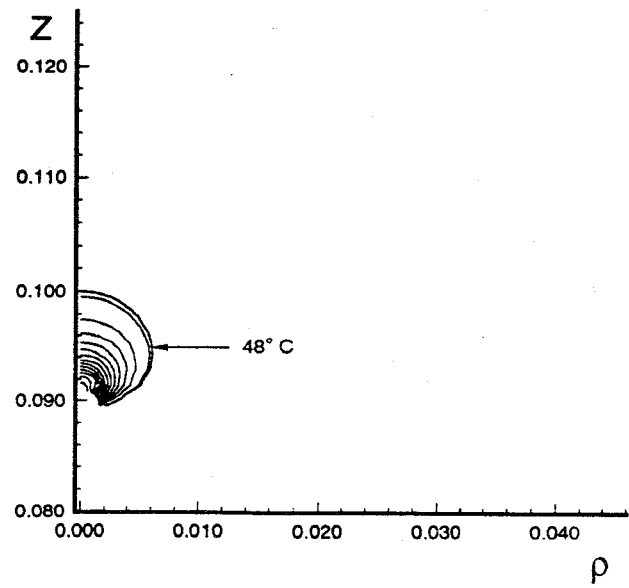


Figure 5: Contour plot of the temperature distribution in the myocardium produced by the RF electrode configuration shown in Figure 3.